

Increased terahertz emission from thermally treated GaSb

S. Winnerl,^{a)} S. Sinning, T. Dekorsy, and M. Helm

Institute of Ion Beam Physics and Materials Research, Forschungszentrum Rossendorf, P.O. Box 510119, D-01314 Dresden, Germany

(Received 9 July 2004; accepted 12 August 2004)

We report on the terahertz (THz) emission from GaSb surfaces with modified surface stoichiometry. While very weak emission is observed from virgin GaSb wafers, the emission is significantly increased by a single thermal treatment of the wafers. Optimum emission is observed for 500 °C thermal annealing. The reason for the THz emission is a surface electric field induced by thermal decomposition of the surface, as corroborated by Raman spectroscopy. © 2004 American Institute of Physics. [DOI: 10.1063/1.1805197]

The generation of short terahertz (THz)-radiation pulses using femtosecond laser pulses has attracted considerable attention in recent years. One mechanism for the generation of THz radiation in semiconductors is the acceleration of photoexcited carriers in the surface field, which is caused by the pinning of the Fermi level at surface states.¹ This mechanism has been explored in a wide variety of materials.² Due to their high efficiency for THz generation InP and GaAs are commonly used. Because of their large energy gap, these materials are not suitable for excitation at the wavelengths of 1.3 or 1.55 μm , where optical-fiber-based lasers can be used. For the small-gap material GaSb ($E_g=0.726$ eV), however, reported THz amplitudes are 35 times smaller than for GaAs surface emitters.² The low efficiency of GaSb surface-field emitters is consistent with the expected small surface field, since the pinning of the Fermi level is close to the valence band.³

Since the surface field is oriented perpendicular to the semiconductor surface, the emission of Hertzian dipole radiation is strongest in the plane of the surface, leading to a poor outcoupling efficiency. Improvements have been achieved by altering the direction of the polarization of photoexcited carriers in magnetic fields^{4–6} and by changing the geometry⁷ or the dielectric environment⁸ of the surface-field emitter. In these recent experiments, the small-gap semiconductors InAs^{4–6} and InGaAs (Ref. 8) have been employed.

In the present study, we used a single thermal treatment to increase the THz emission from GaSb wafers. The samples annealed at 500 °C provided THz field amplitudes comparable to the amplitudes from GaAs surface-field emitters. We used Auger electron spectroscopy (AES) and Raman spectroscopy to analyze the surface. The Raman spectra give evidence for both a decomposition of GaSb during annealing and the presence of a surface electric field in the modified crystals.

Nominally undoped GaSb (p -type, $n=1.2 \times 10^{17} \text{ cm}^{-3}$) samples with a (100) surface orientation were annealed by rapid thermal annealing in the temperature range from 300 to 700 °C for 10 s in N_2 ambient using a face-to-face capping. For the THz emission experiments, the samples were irradiated with femtosecond laser pulses (wavelength 800 nm, pulse duration 50 fs, repetition rate 78 MHz) under the Brewster angle (spot size $\sim 0.16 \text{ mm}^2$). The emitted THz ra-

diation was guided via off-axis parabolic mirrors and focused on a 230- μm -thick ZnTe (110) crystal for electro-optical detection. The 800 nm radiation reflected from the GaSb crystals was blocked using a high-resistivity silicon filter. Fused silica coated with 300 nm indium oxide doped with tin (ITO) was used for combining the THz beam collinearly with a 800 nm probe beam.⁹ The probe beam was transmitted through the ZnTe crystal and a quarter-wave plate. A polarization-sensitive beam splitter was then used to separate the two orthogonal polarization components. The intensity difference $I_1 - I_2$ of these components was measured with photodiodes and a differential amplifier. This signal is proportional to the THz field amplitude in the ZnTe crystal. The temporal resolution was achieved by introducing a calibrated shaker into the laser beam which is focused on the GaSb crystal. Details about electro-optical detection using ZnTe can be found in Refs. 10 and 11. Raman measurements were performed in unpolarized configuration and backscattering geometry (Raman spectrometer HR800, J. Y. Horiba). The wavelength of the excitation light was 523 nm.

The temporal wave forms of the emitted THz pulses from samples annealed at three different temperatures are shown in Fig. 1(a). The wave forms for all temperatures display a minimum followed by a maximum. The minimum in the wave form for the sample annealed at 500 °C is significantly larger than for the samples annealed at 350 and 650 °C. The THz signal size, defined as the difference between the wave-form minimum and its maximum, is shown in Fig. 1(b) versus the annealing temperature. With increasing annealing temperature, the THz signal increases, reaches a maximum for 500 °C and decreases for higher annealing

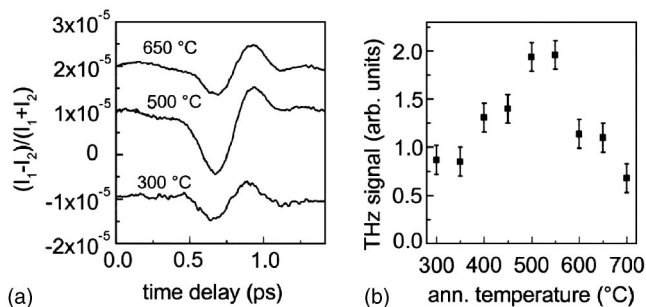


FIG. 1. Temporal wave form of the emitted THz pulses for three different annealing temperatures (a) and dependence of the THz signal on the annealing temperature (b). The curves in (a) are shifted vertically for clarity.

^{a)}Electronic mail: s.winnerl@fz-rossendorf.de

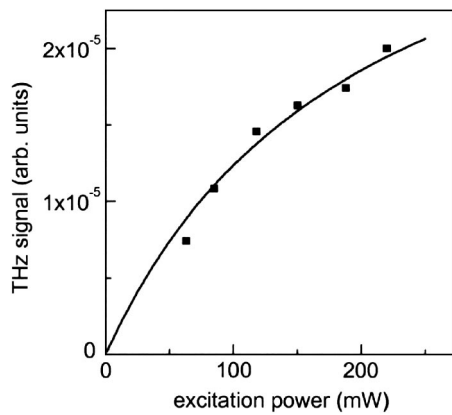


FIG. 2. Dependence of the THz signal on excitation power for the GaSb crystal annealed at 500 °C. 200 mW excitation power corresponds to an optical fluence of $1.4 \mu\text{J}/\text{cm}^2$.

temperatures. The THz signal from the virgin crystal is more than one order of magnitude smaller than the signal for 500 °C annealing temperature. The dependence of the THz emission on the excitation power is shown in Fig. 2 for the GaSb crystal annealed 500 °C. For comparison, THz emission from *n*-doped GaAs ($n=10^{17} \text{ cm}^{-3}$) was studied. The THz wave forms of the GaAs surface-field emitter were reversed in sign compared to the wave forms of the GaSb crystals. This is consistent with a reversed direction of the surface field, as is expected due to the different dopant type. The THz signals from the GaAs surface emitter were 1.5 times larger than the THz emission from the GaSb annealed at 500 °C. Taking into account the electro-optical properties of ZnTe,¹² we calculate the THz field amplitude in the sensor crystal using $E_{\text{THz}}=(I_1-I_2)/(I_1+I_2)c/(\omega n^3 r_{41} d)$, where n is the refractive index, r_{41} the electro-optical coefficient, and d the thickness of the ZnTe crystal,¹² ω is the angular frequency of the probe-beam radiation, and c the speed of light. We obtain THz field amplitudes of 2 and 1.3 V/cm for the GaAs and the GaSb annealed at 500 °C, respectively. For the GaAs emitter, the dependence of the emitted field on the excitation power was linear up to 400 mW, which corresponded to an optical fluence of $2.8 \mu\text{J}/\text{cm}^2$ and an excitation density of $8 \times 10^{16} \text{ cm}^{-3}$. The emission from GaSb annealed at 500 °C, however, deviates from a linear response for excitation powers above 100 mW. Due to the six times larger absorption coefficient of GaSb (Ref. 13) compared to GaAs, the excitation density in GaSb for an excitation power of 100 mW is already $1.2 \times 10^{17} \text{ cm}^{-3}$. This large excitation density, which is similar to the carrier concentration due to the unintentional doping, is responsible for a rapid screening of the surface field. For biased large-aperture THz emitters^{14,15} and for photoconductive antennas,¹⁶ the saturation of THz emission has been described by $E_{\text{THz}} \sim (P/P_0)/[1+(P/P_0)]$, where P is the excitation power and P_0 a characteristic saturation power. We find good agreement between our data and a fit to this dependence for $P_0=200 \text{ mW}$ (solid line in Fig. 2).

In order to explain the increased THz emission from thermally treated GaSb surfaces, we analyzed the samples by different methods. Previously the modification of GaSb surfaces due to thermal treatment has been studied by AES, scanning electron microscopy (SEM) and reflection high-energy electron diffraction,¹⁷ Raman spectroscopy,^{18,19} and electron diffraction.¹⁹ Changes in surface stoichiometry, lat-

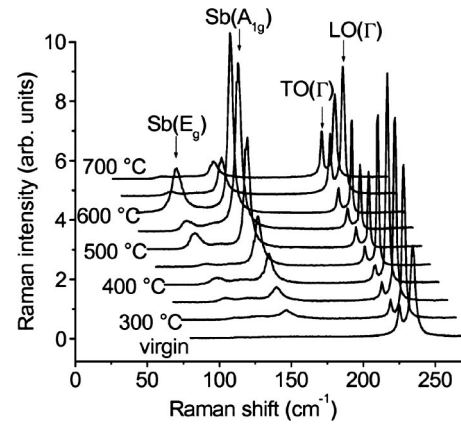


FIG. 3. Raman spectra for the samples annealed at different temperature and the untreated sample (virgin). All measurements were performed on the clear surface.

eral inhomogeneity, and a desorption of Sb at high temperatures have been found.^{17–19} Using optical microscopy and SEM, we found droplets on the surface of the samples annealed at temperatures above 450 °C. The density of the droplets (250 nm^{-2} for 550 °C) decreases with increasing temperature, while their size ($\sim 1 \mu\text{m}$ for 550 °C) increases. Hall measurements yielded *p*-type conduction with a carrier concentration of $1.2 \times 10^{17} \text{ cm}^{-3}$. The Hall mobility of the holes decreases monotonically from $620 \text{ cm}^2/\text{Vs}$ for the lowest annealing temperature to $480 \text{ cm}^2/\text{Vs}$ for 600 °C, indicating the formation of defects at high annealing temperatures.

The Raman spectra for the different annealing temperatures are shown in Fig. 3. The information depth of Raman spectroscopy is defined as $(2\alpha)^{-1}$, where α is the absorption coefficient. For GaSb probed with 523 nm radiation, the information depth is 10 nm.¹³ Raman lines are observed at 115, 150, 225, and 234 cm^{-1} . The lines at 234 and 225 cm^{-1} correspond to the longitudinal optical (LO) and transverse optical (TO) phonon modes, respectively.²⁰ The lines at the lower frequencies, which are not present in the spectrum of the virgin sample, lie in the region where $2\text{TA}(\text{X})$ (114 cm^{-1}) and $\text{LA}(\text{L})$ (155 cm^{-1}) modes exist. However, attributing the observed lines to disorder-induced acoustic modes would pose the question as to why the LO phonon line remains strong and sharp if massive disorder were induced by the annealing process. In addition, one would expect an increase of the TO intensity by disorder. In accordance with Refs. 18,19, we conclude that the lines observed at 115 and 150 cm^{-1} are related to the E_g and A_{1g} Sb–Sb bond vibrations, respectively. This is corroborated by the observation of coherent Sb- A_{1g} phonons in pump-probe experiments (not shown). In Fig. 4(a) the Raman spectrum measured at the clear surface is compared with the Raman spectrum measured on a droplet. The intensity of the Sb-related lines is much stronger on the droplet, while the lines associated with GaSb are weaker, indicating a high crystalline Sb content of the droplets. Furthermore, the TO intensity on the droplet exceeds the LO intensity, which may be due to GaSb that is not well aligned to the (100) substrate. Figure 4(b) shows the dependence of the relative Raman intensities on the annealing temperature, measured on the clean surface. The intensity of the A_{1g} line increases with temperature in the temperature range from 300 to 600 °C. For higher temperatures the inten-

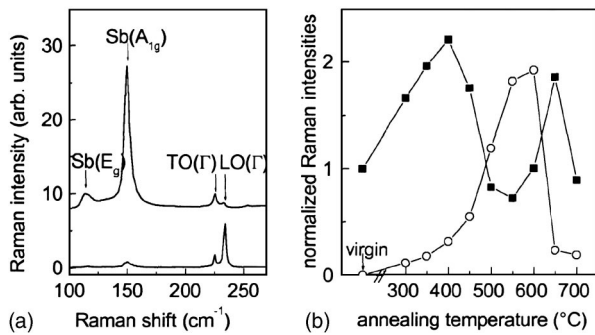


FIG. 4. (a) Raman spectra of the GaSb crystal annealed at 650 °C. For the bottom curve the laser was focused on the clear surface, for the curve shifted upwards it was focused on a droplet. (b) LO phonon Raman intensity of GaSb (full squares) and A_{1g} phonon intensity of Sb (open circles), both normalized to the virgin LO phonon Raman intensity. The lines are guides for the eye.

sity decreases sharply. We attribute the appearance of the Sb modes to a decomposition of the surface of GaSb. The drop in intensity for the highest annealing temperatures can be explained by desorption of Sb from the surface and the formation of Sb-rich droplets. Both the decrease of Sb content in the surface layer for the highest annealing temperature and the high Sb content of the droplets are confirmed by AES data (not shown).

In the annealing temperature range from 400 to 650 °C, a striking anti-correlation of the LO Raman intensity to the A_{1g} Raman intensity is observed. We suggest that this is due to a Sb coverage of the surface that strongly absorbs and reflects the exciting radiation. Hence, the excitation of the underlying GaSb is strongly suppressed. For the annealing temperatures below 500 and for 650 °C, however, the LO phonon intensity is increased compared to the virgin sample. We attribute this increase to electric-field-enhanced Raman scattering, which has been observed in various zinc-blende-type materials.^{21,22} To verify this assumption, we measured the Raman spectra with excitation laser intensities, which were two times and four times larger than the intensity used for the spectra shown in Fig. 2 ($\sim 80 \text{ kW/cm}^2$). By repeating Raman measurements with the original intensity after these experiments, damaging of the samples by the high intensity could be ruled out. While the Raman intensity of the Sb-related peaks and the TO phonon peak were proportional to the excitation laser intensity, a sublinear dependence was observed for the LO Raman intensity from the annealed samples. The deviation from a linear dependence was strongest for the annealing temperature of 500 °C. We attribute this to screening of the surface field by photoexcited carriers. We therefore conclude that the buildup of the surface field with increasing annealing temperature is responsible for the increase of the intensity of the LO phonon line. Both the THz

emission and the intensity dependence of the LO Raman intensity indicate that the surface field is strongest for the annealing temperature of 500 °C. The THz emission from the samples annealed at higher temperatures may be reduced due to a decreased surface field and a reduced carrier mobility caused by defects.

In conclusion, we have observed that the thermally induced decomposition of the surface of GaSb leads to the buildup of a surface field. Thermally treated GaSb can be used as a surface-field THz emitter with an efficiency comparable to a GaAs surface emitter. The small-gap material GaSb has the potential to be used as a surface-field THz emitter in a compact THz source, which is optically excited by an Er^{3+} -doped femtosecond fiber laser.

We thank U. Lucchesi for technical assistance concerning the Raman measurements, H. Reuther for the AES analysis, and A. Kolitsch for fabrication of the ITO coating. We gratefully acknowledge discussions with S. Facsko.

- ¹X.-C. Zhang, B. B. Hu, J. T. Darrow, and D. H. Auston, *Appl. Phys. Lett.* **56**, 1011 (1990).
- ²X.-C. Zhang and D. H. Auston, *J. Appl. Phys.* **71**, 326 (1992).
- ³A. Y. Polyakov, A. G. Milnes, N. B. Smirnov, L. V. Druzhinina, and I. V. Tunitskaya, *Solid-State Electron.* **36**, 1371 (1993).
- ⁴N. Sarukura, H. Ohtake, S. Izumida, and Z. Liu, *J. Appl. Phys.* **84**, 654 (1998).
- ⁵R. McLaughlin, A. Corchia, M. B. Johnston, Q. Chen, C. M. Ciesla, D. D. Arnone, G. A. C. Jones, E. H. Linfield, A. G. Davis, and M. Pepper, *Appl. Phys. Lett.* **76**, 2038 (2000).
- ⁶M. Migita and M. Hangyo, *Appl. Phys. Lett.* **79**, 3438 (2001).
- ⁷M. B. Johnston, D. M. Whittaker, D. Dowd, A. G. Davis, E. H. Linfield, and D. A. Richie, *Opt. Lett.* **27**, 1935 (2002).
- ⁸M. Zedler, C. Janke, P. Haring Bolivar, H. Kurz, and H. Künzel, *Appl. Phys. Lett.* **83**, 4196 (2003).
- ⁹T. Bauer, J. S. Kolb, T. Löffler, E. Mohler, H. G. Roskos, and U. C. Pernisz, *J. Appl. Phys.* **92**, 2210 (2002).
- ¹⁰Q. Wu, M. Litz, and X.-C. Zhang, *Appl. Phys. Lett.* **68**, 2924 (1996).
- ¹¹A. Leitenstorfer, S. Hunsche, J. Shah, M. C. Nuss, and W. H. Knox, *Appl. Phys. Lett.* **74**, 1516 (1999).
- ¹²P. C. M. Planken, H.-K. Nienhuys, H. J. Bakker, and W. T. Wenckebach, *J. Opt. Soc. Am. B* **18**, 313 (2001).
- ¹³D. E. Aspnes and A. A. Studna, *Phys. Rev. B* **27**, 985 (1983).
- ¹⁴J. T. Darrow, X.-C. Zhang, and D. H. Auston, *Appl. Phys. Lett.* **58**, 25 (1991).
- ¹⁵P. K. Benicewicz, J. P. Roberts, and A. J. Taylor, *J. Opt. Soc. Am. B* **11**, 2533 (1994).
- ¹⁶T.-A. Liu, M. Tani, and C.-L. Pan, *J. Appl. Phys.* **93**, 2996 (2003).
- ¹⁷M. Nouaouri, F. W. O. Da Silva, N. Bertura, M. Rouanet, A. Taharaouri, W. Oueini, J. Bonnet, and L. Lassabateri, *J. Cryst. Growth* **172**, 37 (1997).
- ¹⁸S. G. Kim, H. Asahi, M. Seta, J. Takizawa, S. Emura, R. K. Soni, S. Gonda, and T. Tanoue, *J. Appl. Phys.* **74**, 579 (1993).
- ¹⁹C. E. M. Campos and P. S. Pizani, *Appl. Surf. Sci.* **200**, 111 (2002).
- ²⁰M. K. Farr, J. G. Traylor, and S. K. Sinha, *Phys. Rev. B* **11**, 1587 (1975).
- ²¹F. Schäffler and G. Abstreiter, *Phys. Rev. B* **34**, 4017 (1986).
- ²²J. Wagner, A.-L. Alvaez, J. Schmitz, J. D. Ralston, and P. Koidl, *Appl. Phys. Lett.* **63**, 349 (1993).